the case, it must have occurred several centuries ago, as leprosy became increasingly scarce in the British Isles after the 17th century (*3*). It is also conceivable that humans may have been infected through contact with red squirrels bearing *M. leprae*, as these animals were prized for their fur and meat in former times (*30*). Our findings show that further surveys of animal reservoirs of leprosy bacilli are warranted, because zoonotic infection from such reservoirs may contribute to the inexplicably stubborn plateau in the incidence of the human leprosy epidemic despite effective and widespread treatment with multidrug therapy (*1*).

REFERENCES AND NOTES

1. World Health Organization, *Wkly. Epidemiol. Rec.* **88**, 365–379 (2013).
2. H. D. Donoghue *et al.*, *Infect. Genet. Evol.* **31**, 250–256 (2015).
3. V. J. Schuenemann *et al.*, *Science* **341**, 179–183 (2013).
4. A. Alter, A. Grant, L. Abel, A. Alcaïs, E. Schurr, *Mamm. Genome* **22**, 19–31 (2011).
5. S. H. Wong *et al.*, *PLOS Pathog.* **6**, e1000979 (2010).
6. N. Fulton, L. F. Anderson, J. M. Watson, I. Abubakar, *BMJ Open* **6**, e010608 (2016).
7. R. Sharma *et al.*, *Emerg. Infect. Dis.* **21**, 2127–2134 (2015).
8. R. Truman, *Lepr. Rev.* **76**, 198–208 (2005).
9. R. W. Truman *et al.*, *N. Engl. J. Med.* **364**, 1626–1633 (2011).
10. X. Y. Han *et al.*, *Am. J. Clin. Pathol.* **130**, 856–864 (2008).
11. P. Singh *et al.*, *Proc. Natl. Acad. Sci. U.S.A.* **112**, 4459–4464 (2015).
12. M. Carey, G. Hamilton, A. Poole, C. Lawton, *The Irish Squirrel Survey 2007* (COFORD, Dublin, 2007).
13. S. Harris, G. B. Corbet, *The Handbook of British Mammals* (Mammal Society/Blackwell Scientific, ed. 3, 1991).
14. D. M. Tompkins, A. W. Sainsbury, P. Nettleton, D. Buxton, J. Gurnell, *Proc. R. Soc. B* **269**, 529–533 (2002).
15. E. Stokstad, *Science* **352**, 1268–1271 (2016).
16. Council of Europe, Convention on the Conservation of European Wildlife and Natural Habitats (ETS No. 104), Appendix III (1979). https://rm.coe.int/CoERMPublicCommonSearchServices/DisplayDCTMContent?documentId=0900001680304356
17. A. Meredith *et al.*, *Vet. Rec.* **175**, 285–286 (2014).
18. V. Simpson *et al.*, *Vet. Rec.* **177**, 206–207 (2015).
19. See supplementary materials on *Science* Online.
20. J. S. Spencer, P. J. Brennan, *Lepr. Rev.* **82**, 344–357 (2011).
21. J. S. Velarde-Félix, G. Alvarado-Villa, L. Vera-Cabrera, *Am. J. Trop. Med. Hyg.* **94**, 483–484 (2016).
22. L. Vera-Cabrera *et al.*, *J. Clin. Microbiol.* **53**, 1945–1946 (2015).
23. M. Monot *et al.*, *Nat. Genet.* **41**, 1282–1289 (2009).
24. A. J. Drummond, A. Rambaut, *BMC Evol. Biol.* **7**, 214 (2007).
25. B. P. Vieira, C. Fonseca, R. G. Rocha, *Anim. Biodivers. Conserv.* **38**, 49–58 (2015).
26. S. R. Krutzik *et al.*, *Nat. Med.* **9**, 525–532 (2003).
27. C. de Sales Marques *et al.*, *J. Infect. Dis.* **208**, 120–129 (2013).
28. L. B. Adams *et al.*, *Mem. Inst. Oswaldo Cruz* **107** (suppl. 1), 197–208 (2012).
29. P. G. Jessamine *et al.*, *J. Drugs Dermatol.* **11**, 229–233 (2012).
30. P. Lurz, *Red Squirrel: Naturally Scottish* (Scottish Natural Heritage, 2010).

ACKNOWLEDGMENTS

We thank E. Sheehy, E. Goldstein, M. Flaherty, A. Zintl, the National Trust, Forestry Commission Scotland, and Saving Scotland's Red Squirrels for samples, help, and advice. We thank the Genomic Technologies Facility at the University of Lausanne for Illumina sequencing and technical support. Raw sequence read files have been deposited in the Sequence Read Archive of the National Center for Biotechnology Information under accession numbers SRR3672737 to SRR3672758 (NCBI BioProject PRJNA325727), SRR3674396 to SRR3674450 (NCBI BioProject PRJNA325827), SRR3674451 to SRR3674453 (NCBI BioProject PRJNA325856), and SRR3673933; representative TLR1 sequences have been deposited in GenBank under accession numbers KX388139, KX388140, and KX388141. Phylogenetic trees and SNP alignments have been deposited at Treebase under Study Accession URL http://purl.org/phylo/treebase/phylows/study/TB2:S19692. Supported by the Fondation Raoul Follereau and Swiss National Science Foundation grant IZRJZ3_164174 (S.T.C.), the Scottish Government Rural and Environment Science and Analytical Services Division (K.S.), and the Thomas O'Hanlon Memorial Award in Veterinary Medicine (F.McD.).

SUPPLEMENTARY MATERIALS

www.sciencemag.org/content/354/6313/744/suppl/DC1
Materials and Methods
Figs. S1 to S5
Tables S1 to S14
References (*31*–*51*)

21 June 2016; accepted 27 September 2016
10.1126/science.aah3783

ARCTIC SEA ICE

Observed Arctic sea-ice loss directly follows anthropogenic CO_2 emission

Dirk Notz[1]* and Julienne Stroeve[2,3]

Arctic sea ice is retreating rapidly, raising prospects of a future ice-free Arctic Ocean during summer. Because climate-model simulations of the sea-ice loss differ substantially, we used a robust linear relationship between monthly-mean September sea-ice area and cumulative carbon dioxide (CO_2) emissions to infer the future evolution of Arctic summer sea ice directly from the observational record. The observed linear relationship implies a sustained loss of 3 ± 0.3 square meters of September sea-ice area per metric ton of CO_2 emission. On the basis of this sensitivity, Arctic sea ice will be lost throughout September for an additional 1000 gigatons of CO_2 emissions. Most models show a lower sensitivity, which is possibly linked to an underestimation of the modeled increase in incoming longwave radiation and of the modeled transient climate response.

The ongoing rapid loss of Arctic sea ice has far-reaching consequences for climate, ecology, and human activities alike. These include amplified warming of the Arctic (*1*), possible linkages of sea-ice loss to mid-latitude weather patterns (*2*), changing habitat for flora and fauna (*3*), and changing prospects for human activities in the high north (*3*). To understand and manage these consequences and their possible future manifestation, we need to understand the sensitivity of Arctic sea-ice evolution to changes in the prevailing climate conditions. However, assessing this sensitivity has been challenging. For example, climate-model simulations differ widely in their timing of the loss of Arctic sea ice for a given trajectory of anthropogenic CO_2 emissions: Although in the most recent Climate Model Intercomparison Project 5 (CMIP5) (*4*), some models project a near ice-free Arctic during the summer minimum already toward the beginning of this century, other models keep a substantial amount of ice well into the next century even for an external forcing based on largely undamped anthropogenic CO_2 emissions as described by the Representative Concentration Pathway scenario RCP8.5 (*4*, *5*).

To robustly estimate the sensitivity of Arctic sea ice to changes in the external forcing, we identify and examine a fundamental relationship in which the CMIP5 models agree with the observational record: During the transition to a seasonally ice-free Arctic Ocean, the 30-year running mean of monthly mean September Arctic sea-ice area is almost linearly related to cumulative anthropogenic CO_2 emissions (Fig. 1). In the model simulations, the linear relationship holds until the 30-year running mean, which we analyze to reduce internal variability, samples more and more years of a seasonally ice-free Arctic Ocean, at which point the relationship levels off toward zero. For the first few decades of the simulations, a few models simulate a near-constant sea-ice cover despite slightly rising cumulative CO_2 emissions. This suggests that in these all-forcing simulations, greenhouse-gas emissions were initially not the dominant driver of sea-ice evolution. This notion is confirmed by the CMIP5 1% CO_2 simulations, where the initial near-constant sea-ice cover does not occur (fig. S3A). With rising greenhouse-gas emissions, the impact of CO_2 becomes dominating also in all all-forcing simulations, as evidenced by the robust linear trend that holds in all simulations throughout the transition period to seasonally ice-free conditions. We define this transition period as starting when the 30-year mean September Arctic sea-ice area in a particular simulation decreases for the first time to an area that is 10% or more below the simulation's minimum sea-ice cover during the period 1850 to 1900, and

[1]Max Planck Institute for Meteorology, Hamburg, Germany. [2]National Snow and Ice Data Center, Boulder, CO, USA. [3]University College, London, UK.
*Corresponding author. Email: dirk.notz@mpimet.mpg.de

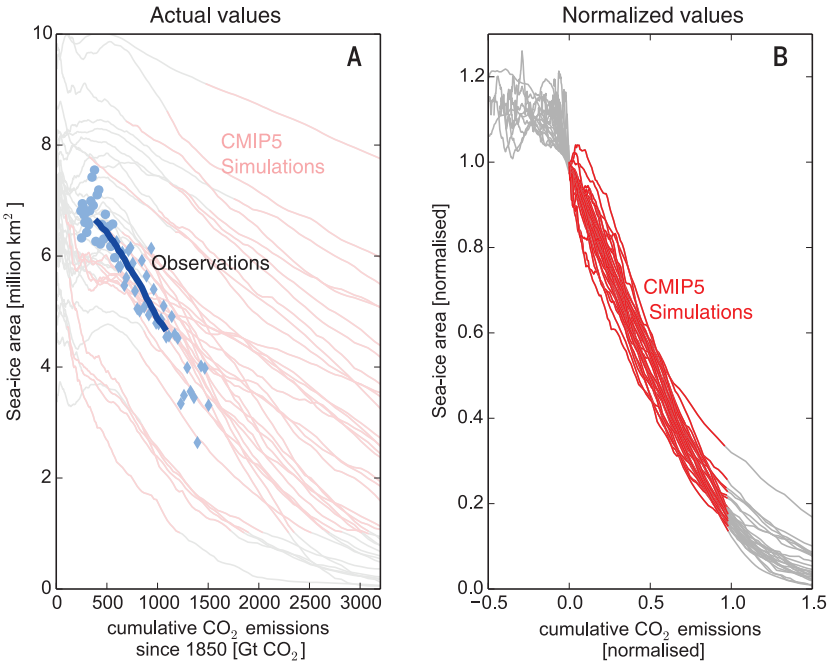

Fig. 1. Relationship between September Arctic sea-ice area and cumulative anthropogenic CO_2 emissions. (**A**) Actual values. The thick blue line shows the 30-year running mean of observed September sea-ice area, and the thinner red lines the 30-year running means from CMIP5 model simulations. For reference, we also show the annual values of observed September sea-ice area, based from 1953 to 1978 on HadISST (*31*) (circles) and from 1979 to 2015 on the NSIDC sea-ice index (*32*) (diamonds; see methods for details). (**B**) Normalized simulations. For this plot, the simulated CMIP5 sea-ice area is normalized by dividing by the simulated sea-ice area at the onset of the transition period as defined in the text. For each simulation, the cumulative emissions (*33*) are set to 0 at the onset of the transition period and then linearly scaled to reach 1 by the end of the transition period (compare table S1 for actual values). This linearization is only carried out to more explicitly visualize the linearity in the models. All analyses in the paper are based on the original data shown in (A).

as ending once the 30-year mean September Arctic sea-ice area drops for the first time below 1 million km^2 (see table S1 for specific numbers).

The existence of a robust, linear relationship between cumulative CO_2 emissions and Arctic sea-ice area in all CMIP5 models and in the observational record extends the findings of earlier studies that demonstrated such relationships for individual, sometimes more simplified models (*6*, *7*), and of studies that have demonstrated a linear relationship between Arctic sea-ice area and either global mean temperature (*5*, *8*–*12*) or atmospheric CO_2 concentration (*13*, *14*). These linear relationships are highly suggestive of a fundamental underlying mechanism, which has been elusive so far. We will later suggest a conceptual explanation of the linearity, but we begin by discussing two implications of the observed linear relationship that are independent of its underlying mechanism.

First, the observed linear relationship allows us to estimate a sensitivity of 3.0 ± 0.3 m^2 of September Arctic sea-ice loss per metric ton of anthropogenic CO_2 emissions during the observational period 1953 to 2015. This number is sufficiently intuitive to allow one to grasp the contribution of personal CO_2 emissions to the loss of Arctic sea ice. For example, on the basis of the observed sensitivity, the average personal CO_2 emissions of several metric tons per year can be directly linked to the loss of tens of square meters of Arctic sea ice in every year (fig. S1).

Second, the linear relationship allows for a robust evaluation of climate-model simulations. Although a number of previous studies have found that the observed sea-ice retreat has been faster than projected by most climate-model simulations (*15*, *16*), it has remained unclear whether these differences are primarily a manifestation of internal variability (*17*, *18*). The sensitivity that we estimate here is, in contrast, based on the average evolution over many decades, thus eliminating internal variability to a substantial degree. A mismatch between the observed and the simulated sensitivity hence robustly indicates a shortcoming either in the model or in the external forcing fields used for a simulation.

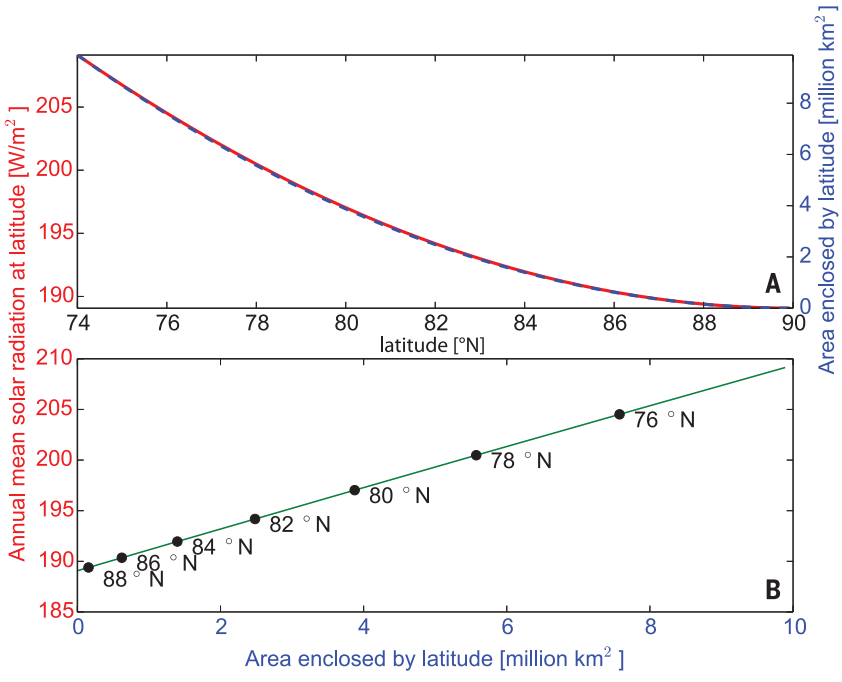

Fig. 2. Relationship between annual mean incoming shortwave radiation and sea-ice area. (**A**) Annual mean incoming top-of-the-atmosphere shortwave radiation at, and area within, a given latitude. The area within a given latitude band is calculated from simple spherical geometry. The latitudinal dependence of average daily incoming shortwave radiation at the top of the atmosphere is calculated from the very good approximation $S(\varphi) = 1 - 0.482P_2(\sin(\varphi))$, where P_2 is the second Legendre polynom (*34*). (**B**) As in (A), but with the *x* axis exchanged for clarity.

Evaluating the simulated sensitivity, we find that most CMIP5 models systematically underestimate the observed sensitivity of Arctic sea ice relative to anthropogenic CO_2 emissions of 3.0 ± 0.3 m^2 (see table S1 for details). Across the full

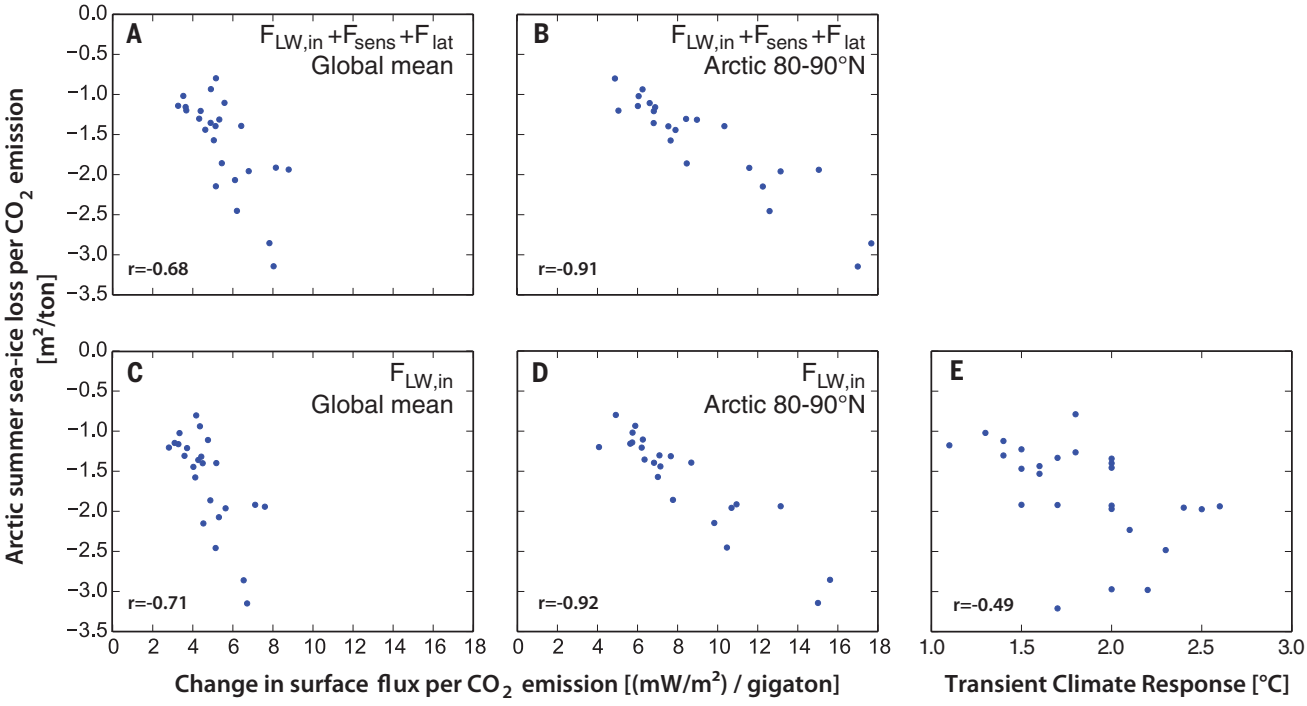

Fig. 3. Relationship between Arctic sea-ice loss and other metrics. (**A**) Each dot represents the sensitivity of Arctic sea-ice loss in a particular model as a function of the increase in global mean incoming nonshortwave fluxes per CO_2 emission in the same model. The latter was obtained from a linear fit of incoming nonshortwave fluxes as a function of cumulative anthropogenic CO_2 emissions during the transition period of each individual model. (**B**) Same as (A), but fluxes only evaluated in the Arctic. (**C** and **D**) Same as (A) and (B), but neglecting sensible and latent heat fluxes. (**E**) Each dot represents the sensitivity of Arctic sea-ice loss in a particular model as a function of the transient climate response (*24*) in the same model. [See table S1 for actual values and supplementary text for more discussion on (E).] All correlations given in the figure are significant at the 1% level.

transition range to near ice-free conditions, the multimodel mean sensitivity is only 1.75 ± 0.67 m^2 loss of Arctic sea ice per metric ton of anthropogenic CO_2 emissions. Because of the linear response, a similar sensitivity is obtained for subperiods of the transition period that have the same length as our observational record, with overall maximum sensitivities over such 61-year-long time periods from individual simulations of 1.95 ± 0.70 m^2/ton. These estimates of the models' sensitivity might be biased somewhat high, as previous studies found that the aerosol forcing of CMIP5 simulations might have been too weak in recent decades (*19*, *20*). This would give rise to artificially amplified warming and thus amplified sea-ice loss in these simulations, rendering the true sensitivity of the models to be even lower than the values that we estimate here.

The low sensitivity of the modeled sea-ice response can be understood through a conceptual model that explains the linearity. To derive such a conceptual model, we consider the annual mean surface energy balance at the ice edge, which describes the fact that the net incoming shortwave radiation $(1-\alpha)F_{SW}$ and the incoming nonshortwave flux $F_{nonSW,in}$ are balanced by the outgoing nonshortwave flux and the conductive heat flux at the surface of the ice.

With increasing atmospheric CO_2 concentration, the incoming nonshortwave flux increases at the ice edge in response to the rising atmospheric emissivity and related atmospheric feedbacks. However, neither the outgoing nonshortwave flux nor the conductive heat flux in the ice will change much, as the surface properties of sea ice at the ice edge are largely independent of its location. We conjecture that this also holds for total albedo α, because a possible rise in cloudiness caused by sea-ice loss (*21*) will primarily occur over the open water south of the moving ice edge, rather than at the ice edge itself. In addition, the albedo of clouds is comparable to that of the ice at the ice edge. Hence, it seems plausible to assume that the surface energy balance at the ice edge is primarily kept closed by a decrease in the incoming shortwave flux that compensates for the increase in incoming nonshortwave flux. Such decrease of the incoming shortwave radiation is obtained by the northward movement of the ice edge to a region with less annual mean solar irradiance. Equilibrium is reestablished at the ice edge when

$$\Delta F_{SW}(1-\alpha) = -\Delta F_{nonSW,in} \quad (1)$$

If, for simplicity, we assume a circular shape of the sea-ice cover centered at the North Pole, the sea-ice area that is enclosed by any given latitude has nearly the same latitudinal dependence as the annual mean incoming shortwave radiation at the top of the atmosphere (Fig. 2A). Hence, the change in area enclosed by the ice edge ΔA_{seaice} should be roughly proportional to the change in incoming annual mean shortwave radiation at the ice edge (Fig. 2B)

$$\Delta A_{seaice} \propto \Delta F_{SW}(1-\alpha) \quad (2)$$

We additionally find empirically that the incoming nonshortwave flux is fairly linearly related to anthropogenic CO_2 emissions E_{CO_2} across CMIP5 model simulations both in the Arctic, where the loss of sea ice might amplify the change in radiative forcing, and globally, where such amplification is small (fig. S2). The linearity arises because more of each ton of emitted CO_2 remains in the atmosphere as oceanic CO_2 uptake decreases in the future. This then roughly compensates for the logarithmic rather than linear change of atmospheric longwave emission with changes in atmospheric CO_2 concentration (*22*). It is hence a plausible assumption that the linearity of incoming longwave radiation with rising CO_2 emissions also holds at the ice edge, which we can express as

$$\Delta F_{nonSW,in} = \frac{dF_{nonSW,in}}{dE_{CO_2}} \Delta E_{CO_2} \quad (3)$$

Inserting Eqs. 2 and 3 into Eq. 1 then finally gives

$$\Delta A_{seaice} = \frac{dF_{nonSW,in}}{dE_{CO_2}} \Delta E_{CO_2} \quad (4)$$

which for constant $dF_{nonSW,in}/dE_{CO_2}$ is a possible explanation for the observed linear relationship

between Arctic sea-ice area and cumulative CO_2 emission.

On the basis of this expression, we can infer that most climate models underestimate the loss of Arctic sea ice because they underestimate the increase of incoming nonshortwave flux for a given increase of anthropogenic CO_2 emissions. An analysis of the available fields of surface heat fluxes in the CMIP5 archive confirms this notion, with high correlation between modeled sea-ice sensitivity and modeled changes in either incoming total nonshortwave flux or incoming longwave radiation, as the latter dominates the change in the nonshortwave flux (Fig. 3, A to D). Unfortunately, observational uncertainty is currently too large to test our finding of a lower-than-expected increase in incoming longwave radiation against independent records (*23*).

On a more regional scale, our conceptual explanation allows us to ascribe a minor role for the overall evolution of sea ice to processes that are unrelated to the large-scale change in atmospheric forcing. This includes a minor role of oceanic heat transport on the time scales that we consider here, because we can derive a linear relationship without considering these transports. Although it might alternatively be possible that the oceanic heat transports have changed monotonously in recent decades, we have no indication that this is the case from either observations or model simulations. The current minor role of oceanic heat transports implies that on time scales of several centuries, the linearity will most likely no longer hold, because sensitivity will increase once changes in oceanic heat content start measurably affecting Arctic sea-ice coverage (*12*).

Our results also suggest that regional differences in atmospheric heat-flux convergence or wind forcing do not appreciably affect the Arctic-wide mean energy balance on the time scales that we consider here. Furthermore, this also explains why the linear relationship does not hold in the Antarctic, where dynamical forcing from wind and oceanic heat transport are key drivers of the large-scale sea-ice evolution.

The apparent minor role of oceanic heat transport, and the correlation between the change in global surface fluxes and Arctic sea-ice loss, suggest that we can use the observed evolution of Arctic sea ice as an emergent constraint on transient climate response (TCR). This is commonly defined as the global-mean warming at the time of doubled atmospheric CO_2 concentration after a 1% CO_2 increase per year (*24*). Indeed, we find good correlation between the modeled sea-ice sensitivity and TCR both in the full-forcing simulations (Fig. 3E) and in the simulations with rising CO_2 only (fig. S3B).

Unfortunately, though indicative of a TCR at the higher end of simulated values, the correlation does not allow for a direct estimate of TCR for two reasons: (i) The loss of Arctic sea ice is more directly driven by the regional temperature rise in the Arctic than by the global temperature rise that is expressed by the TCR. Any failure of the models to realistically simulate the ratio between global and Arctic temperature rise, usually referred to as Arctic amplification, could hence lead to an erroneous quantitative estimate of the TCR based on the correlation that we identify. (ii) TCR is estimated from simulations where all non-CO_2 forcings are kept constant, whereas the non-CO_2 forcings change in the historical and RCP8.5 simulations that we consider here. This affects, at least to some degree, the robustness of the correlation (see supplementary text for details).

Previous studies that estimated climate sensitivity from emergent constraints have usually focused on the equilibrium climate sensitivity (ECS), which describes the equilibrium global-mean warming for a sustained doubling of atmospheric CO_2 concentration. They also come to the conclusion that the real sensitivity of the Earth climate system is at the higher end of simulated values, from analyzing either atmospheric convective mixing (*25*) or mid-troposphere relative humidity (*26*). By contrast, studies analyzing the Earth's energy budget, particularly after considering the recent slowing in atmospheric warming, find that the TCR should be at the lower end of simulated values (*27*, *28*). This result, however, might be biased by the different data coverage in models and observations (*29*).

Regarding the future evolution of sea ice, our analysis suggests that there is little reason to believe that the observed sensitivity of Arctic sea-ice loss will change substantially in the forseeable future. Hence, we can directly estimate that the remainder of Arctic summer sea ice will be lost for roughly an additional 1000 Gt of CO_2 emissions on the basis of the observed sensitivity of 3.0 ± 0.3 m^2 September sea-ice loss per ton of anthropogenic CO_2 emissions. Because this amount is based on the 30-year running mean of monthly averages, it is a very conservative estimate of the cumulative emissions at which the annual minimum sea-ice area drops below 1 million km^2 for the first time. In addition, internal variability causes an uncertainty of around 20 years as to the first year of a near-complete loss of Arctic sea ice (*18*, *30*). For current emissions of 35 Gt CO_2 per year, the limit of 1000 Gt will be reached before mid-century. However, our results also imply that any measure taken to mitigate CO_2 emissions will directly slow the ongoing loss of Arctic summer sea ice. In particular, for cumulative future total emissions compatible with reaching a 1.5°C global warming target—i.e., for cumulative future emissions appreciably below 1000 Gt—Arctic summer sea ice has a chance of long-term survival, at least in some parts of the Arctic Ocean.

REFERENCES AND NOTES

1. F. Pithan, T. Mauritsen, *Nat. Geosci.* **7**, 181–184 (2014).
2. T. Vihma, *Surv. Geophys.* **35**, 1175–1214 (2014).
3. W. N. Meier *et al.*, *Rev. Geophys.* **52**, 185–217 (2014).
4. K. E. Taylor, R. J. Stouffer, G. A. Meehl, *Bull. Am. Meteorol. Soc.* **93**, 485–498 (2012).
5. J. Stroeve, D. Notz, *Global Planet. Change* **135**, 119–132 (2015).
6. K. Zickfeld, V. K. Arora, N. P. Gillett, *Geophys. Res. Lett.* **39**, L05703 (2012).
7. T. Herrington, K. Zickfeld, *Earth Syst. Dyn.* **5**, 409–422 (2014).
8. J. M. Gregory *et al.*, *Geophys. Res. Lett.* **29**, 28-1–28-4 (2002).
9. M. Winton, *J. Clim.* **24**, 3924–3934 (2011).
10. I. Mahlstein, R. Knutti, *J. Geophys. Res.* **117**, D06104 (2012).
11. J. K. Ridley, J. A. Lowe, H. T. Hewitt, *Cryosphere* **6**, 193–198 (2012).
12. C. Li, D. Notz, S. Tietsche, J. Marotzke, *J. Clim.* **26**, 5624–5636 (2013).
13. O. Johannessen, *Atmos. Ocean. Sci. Lett.* **1**, 51 (2008).
14. D. Notz, J. Marotzke, *Geophys. Res. Lett.* **39**, L051094 (2012).
15. F. Massonnet *et al.*, *Cryosphere* **6**, 1383–1394 (2012).
16. J. C. Stroeve *et al.*, *Geophys. Res. Lett.* **39**, L16502 (2012).
17. G. Flato *et al.*, in *Climate Change 2013: The Physical Science Basis. Contribution of Working Group I to the Fifth Assessment Report of the Intergovernmental Panel on Climate Change*, T. Stocker *et al.*, Eds. (Cambridge Univ. Press, 2013), chap. 9, pp. 741–866.
18. D. Notz, *Philos. Trans. R. Soc. A* **373**, 20140164 (2015).
19. B. D. Santer *et al.*, *Nat. Geosci.* **7**, 185–189 (2014).
20. G. A. Schmidt, D. T. Shindell, K. Tsigaridis, *Nat. Geosci.* **7**, 158–160 (2014).
21. I. V. Gorodetskaya, L.-B. Tremblay, B. Liepert, M. A. Cane, R. I. Cullather, *J. Clim.* **21**, 866–882 (2008).
22. H. D. Matthews, N. P. Gillett, P. A. Stott, K. Zickfeld, *Nature* **459**, 829–832 (2009).
23. G. L. Stephens *et al.*, *Nat. Geosci.* **5**, 691–696 (2012).
24. U. Cubasch *et al.*, in *Climate Change 2001: The Scientific Basis*, J. T. Houghton *et al.*, Eds. (Cambridge Univ. Press, 2001), chap. 9, pp. 525–582.
25. S. C. Sherwood, S. Bony, J.-L. Dufresne, *Nature* **505**, 37–42 (2014).
26. J. T. Fasullo, K. E. Trenberth, *Science* **338**, 792–794 (2012).
27. A. Otto *et al.*, *Nat. Geosci.* **6**, 415–416 (2013).
28. N. P. Gillett, V. K. Arora, D. Matthews, M. R. Allen, *J. Clim.* **26**, 6844–6858 (2013).
29. M. Richardson, K. Cowtan, E. Hawkins, M. B. Stolpe, *Nat. Clim. Chang.* **6**, 931–935 (2016).
30. A. Jahn, J. E. Kay, M. M. Holland, D. M. Hall, *Geophys. Res. Lett.* **43**, 9113–9120 (2016).
31. Hadley Center for Climate Prediction and Research, Met Office, HadISST 1.1 - global sea-ice coverage and sea surface temperature (1870-2015); NCAS British Atmospheric Data Centre (2006); http://badc.nerc.ac.uk/data/hadisst/.
32. F. Fetterer, K. Knowles, W. Meier, M. Savoie, Sea ice index, Digital media, National Snow and Ice Data Center, Boulder, CO (2002, updated 2014).
33. M. Meinshausen *et al.*, *Clim. Change* **109**, 213–241 (2011).
34. G. R. North, *J. Atmos. Sci.* **32**, 2033–2043 (1975).

ACKNOWLEDGMENTS

We are grateful to J. Marotzke for the suggestion to analyze the TCR and for helpful comments on the manuscript. We are also grateful to two anonymous reviewers, whose insightful comments were essential for framing the final version of our study. We further thank B. Soden, D. Olonscheck, and C. Li for helpful feedback. D.N. acknowledges funding through a Max Planck Research Fellowship. J.S. acknowledges funding from NASA grant NNX12AB75G and NSF grant PLR 1304246. All primary data used for this study are based on publicly available output from CMIP5 models and are also available upon request from publications@mpimet.mpg.de.

SUPPLEMENTARY MATERIALS

www.sciencemag.org/content/354/6313/747/suppl/DC1
Materials and Methods
Supplementary Text
Figs. S1 to S3
Table S1
References (*35*–*37*)

27 May 2016; accepted 12 October 2016
Published online 3 November 2016
10.1126/science.aag2345